Pergamon

J. Quant. Spectrosc. Radiat. Transfer Vol. 52, No. 5, pp. 677–691, 1994
Elsevier Science Ltd. Printed in Great Britain

0022-4073(94)00068-9

A COOLABLE LONG PATH ABSORPTION CELL FOR LABORATORY SPECTROSCOPIC STUDIES OF GASES

J. BALLARD,†‡ K. STRONG,§¶ J. J. REMEDIOS,§ M. PAGE,† and W. B. JOHNSTON†‖

†E.P.S.R.C. Rutherford Appleton Laboratory, Chilton, Oxfordshire and §Clarendon Laboratory, University of Oxford, Parks Road, Oxford, U.K.

(Received 13 July 1993; received for publication 20 May 1994)

Abstract—A long path absorption cell (Long White Cell) which has been designed and built for laboratory spectroscopic studies of gases found in terrestrial and planetary atmospheres is described. Factors influencing the design and construction are discussed, including aspects of the optical, mechanical, cryogenic, vacuum, gas handling and safety systems, and the pressure and temperature monitoring systems. The practical capabilities of the cell include absorber pathlengths up to 512 m, gas sample pressures up to 5 bar and temperatures between 190 and 300 K, and the suitability for use with corrosive and flammable gases. The performance of the cell is discussed in relation to spectroscopic measurements of mixtures of gaseous methane and hydrogen.

1. INTRODUCTION

The Long White Cell (LWC) is a multiple-pass gas absorption cell designed for spectroscopy of flammable, toxic, and corrosive gases. The primary purpose of the cell is to allow recording of gas phase spectra (over a wide range of pathlengths, temperatures, and pressures) relevant to remote sensing of the terrestrial and planetary atmospheres. It has been installed at the Rutherford Appleton Laboratory; this paper describes that installation and the interfaces to a Bomem DA3.002 Fourier transform spectrophotometer. A number of long path cells have been reported but some were operated at room temperature only (e.g., Bernstein and Herzberg,[1] and Stephens[2]) or at a limited number of fixed temperatures dictated by available cryogens (e.g., Blickensderfer et al[3] and McKeller et al[4]). By contrast the cell reported here can be operated at any temperature within a wide range in a manner similar to the cells reported by Horn and Pimentel,[5] Le Doucen et al,[6] Shetter et al,[7] Kim et al,[8] and Briesmeister et al.[9]

2. THE OPTICAL DESIGN OF THE LWC

The optical system used in the LWC is similar to that first described by White,[10] consisting of three concave spherical mirrors of identical radius of curvature which allow long optical pathlengths to be obtained in a cell of much shorter physical length. A side extension (tab) is included in the design of the field mirror so that the number of non-overlapping images which can be stacked across the field mirror is double that achievable with the simple White design, as discussed by Bernstein and Herzberg.[1] The considerations which led to the design shown in Fig. 1 are discussed below.

The cell was interfaced optically to the spectrometer using reflective transfer optics, and the optical design of the cell was considered in conjunction with the design of these optics and of the spectrometer. The transfer optics formed an image of a field-limiting iris located inside the spectrometer at a point in the LWC which corresponded to the input image for the cell (see Fig. 1).

‡To whom all correspondence should be addressed.
¶Present address: Centre for Atmospheric Chemistry, York University, North York, Ontario, Canada M3J 1P3.
‖Present address: AEA Technology, Harwell, U.K.

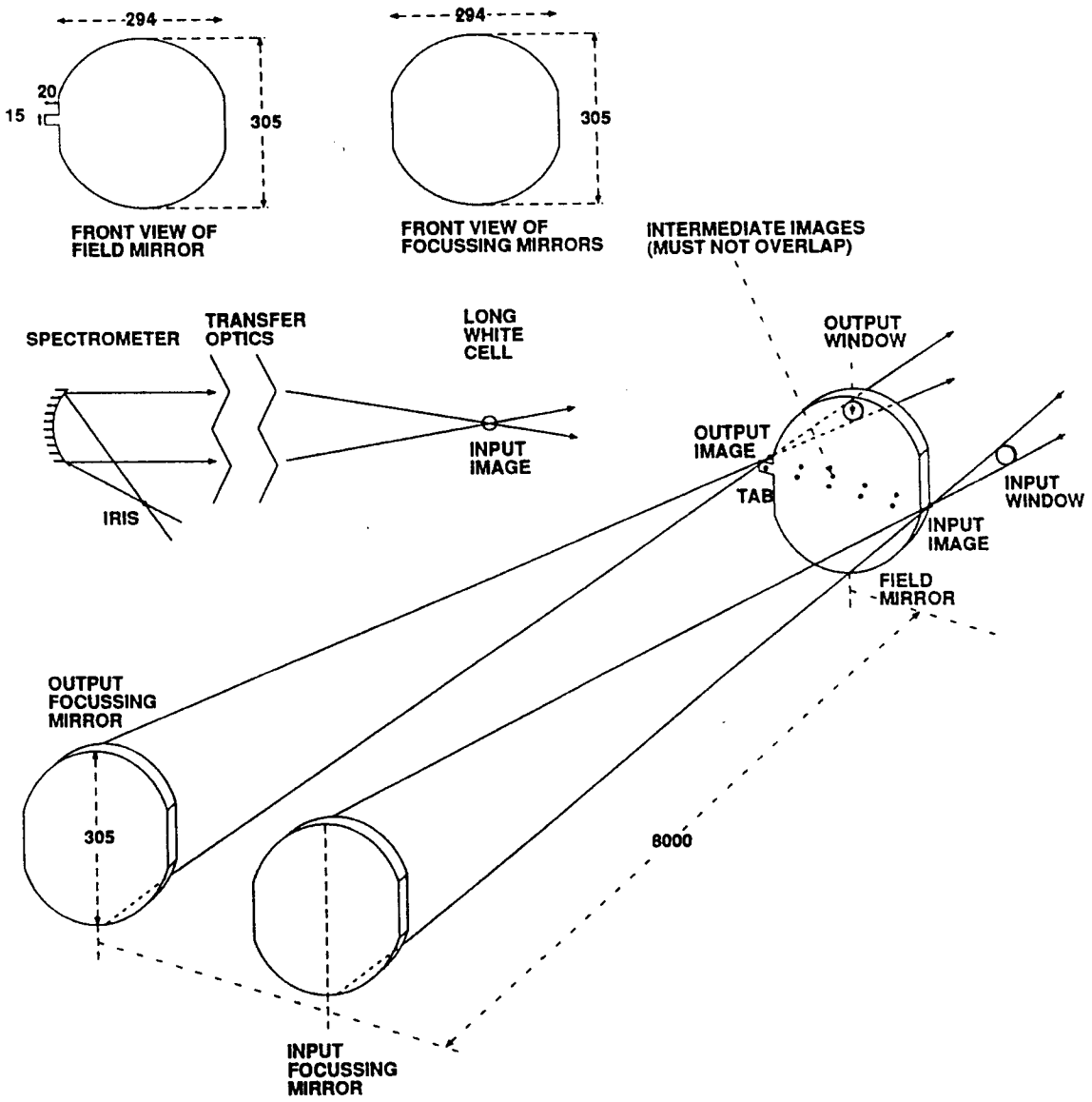

Fig. 1. Schematic diagram of the LWC optics and the interface to the spectrometer.

The transfer optics were imaging, so the quantity $A\Omega$ (where A is the beam diameter and Ω is the solid angle of rays in the beam) was conserved through the system. The $A\Omega$ for radiation at the spectrometer iris was determined by the size of the iris aperture (a compromise choice between throughput and spectral resolution) and the f-number of the interferometer collimator. With a suitable choice of mirrors in the transfer optics both the A and the Ω of radiation at the input to the LWC could be specified. The overall design, however, also included the physical dimensions of the cell and its mirrors, since the Ω for radiation entering the cell should be matched to the f-number of the input focussing mirror, and the diameter of the input image determined the maximum number of images which can be accommodated on the field mirror without adjacent images overlapping. The latter criterion was important if there was to be a unique absorption pathlength. Furthermore, the radius of curvature of the cell mirrors determined the physical length of the cell and the number of reflections required for a given absorber pathlength.

The final design was derived by considering the above in conjunction with constraints imposed by the space available for the complete installation. This led to a system using gold-coated mirrors having an 8 m radius of curvature and a 305 mm diameter, as shown in Fig. 1. The theoretical pathlengths and throughputs attainable in the mid-i.r., for given iris sizes set in the spectrometer,

Table 1. Table showing pathlength and throughput parameters for differing spectrometer iris sizes.

iris dia. (mm)	input image dia. (mm)	No of images (no over-lap)	No of Reflections	Theoretical Maximum Path (m)	Throughput at maximum path	Max Path at t'put = 20% (m)
0.5	3.3	177	355	2848	0.00077	640
1.0	6.6	89	179	1440	0.027	640
2.0	13.2	45	91	736	0.16	640
4.0	26.4	23	47	384	0.39	384

are given in Table 1. In this table, the second column gives the diameter of the input image in the LWC for a given spectrometer iris aperture, assuming that the collimating mirror in the spectrometer is 76 mm diameter with a focal length of 305 mm, and that the radiation exactly fills the input focussing mirror in the LWC. The third column gives the maximum number of non-overlapping images which can be placed on the single mirror in two rows, obtained by dividing the width of the mirror (294 mm) by the input image diameter. The total number of reflections is given by $2n + 1$, where n is the number of images, and the theoretical maximum pathlength is given by $(2n + 2) \times 8$ m. This table neglects the 0.75 m path which corresponds to twice the distance from the i.r. windows to the front surface of the single mirror. Column 6 indicates the losses due to reflections, assuming that each reflection is 98% efficient, while column 7 gives an estimate of the maximum useable path if reflective losses are not to exceed 80%. The above assumes perfect geometric imagery and neglects diffraction effects. However, the latter must be taken into account at longer wavelengths, for example in the far-i.r.

The mirrors were held in kinematic mounts which were designed to provide support with minimal distortion of the reflecting surface. Each mirror could be adjusted from outside the LWC when the latter was evacuated or filled with absorber gas, at any temperature. Such adjustments were found to be essential both for pathlength changes and to compensate for distortions and flexures of the cell which take place when the system was evacuated and cooled. Tilt adjustments about both horizontal and vertical axes were provided for all mirrors, and the focussing mirrors could also be moved along the longitudinal axis of the cell. The adjustments were achieved by simple rotation of control rods which passed through the inner and outer end plates and which interlocked with pivot, lever and spring mechanisms at the back of the mirrors. The control rods which passed through the outer end plate could be retracted and disengaged from those which passed through the inner cell in order to minimise thermal losses and undesirable mechanical coupling to the mirror mounts during operations with the absorption cell cold.

The optical system also included windows through which the i.r. radiation passed, and viewing windows through which the images on the field mirror could be observed during optical alignment. The transmittance of the windows and the reflectance of the mirrors determined the spectral range over which the cell could be used.

3. THE MECHANICAL DESIGN OF THE LWC

The mechanical design for the LWC was influenced by the range of gas pressures and temperatures over which the cell was to be operated, the space available in which to install the cell, the optical design discussed above, and the desire to have a system in which corrosive gases could be used. These considerations led to a design consisting of two concentric stainless steel cylindrical cells, each with removable endplates. The inner cell formed the absorption volume which contained the multi-pass mirrors and into which the gas under investigation was introduced; the outer cell served to provide a vacuum space for thermal isolation. The outer cell was 9000 mm long, had an internal diameter of 1000 mm, and was mounted on a support frame whose feet were bonded to anti-vibration pads. The endplates of the outer cell were flat stainless steel plates 25 mm thick, reinforced by ribs welded to the inside face, and included ports for the viewing and i.r. windows, the mirror adjustors, and a gas feedthrough.

Welded at fixed points along the inside of the outer cell were two rails which supported the inner cell. This cell was 8635 mm in length, 750 mm in internal diameter, and 3.81 m^3 in volume, which made the volume of the vacuum annulus 3.25 m^3. The inner cell was designed for a maximum working pressure of 5 bar over the temperature range 80–300 K, though the lowest temperature to which the cell has been cooled to date is 190 K. The inner cell was mounted on PTFE-insulated support feet welded to its outer surface, which positioned it concentrically within the outer cell and allowed movement when the inner cell contracted or expanded. A PTFE-insulated bracket, bolted to the inner cell endplate at the single-mirror end, and welded to one of the outer cell support rails, positioned the inner cell axially and kept its single mirror end fixed during contraction and expansion. The endplates for the inner cell were 38 mm thick, also reinforced by ribs on the inside face and including ports equivalent to those on the outer cell endplates.

4. THE VACUUM AND GAS HANDLING SYSTEMS

The vacuum and gas handling systems used in conjunction with the LWC during the work described in Ref. 11 are shown schematically in Fig. 2, and were needed to fulfil the following functions:

(1) Maintaining a high vacuum in the outer annulus space for thermal isolation of the inner absorption cell.
(2) Enabling the inner absorption cell to be evacuated to a low pressure prior to filling with the gas to be studied.
(3) Enabling the inner cell to be filled in a safe manner with a flammable gas mixture of known mixing ratio and total pressure.
(4) Evacuating the inner cell safely after recording a set of spectra.

The main vacuum system comprised two rotary pumps, a 30 cm oil diffusion pump and a 30 cm turbo-molecular pump. The latter maintained a high vacuum in the outer cell, while the former was used to evacuate the inner cell. Both systems were fitted with refrigerated baffles to reduce backstreaming and pressures below 10^{-5} torr could easily be maintained in both the outer and the inner cells. To ensure adequate performance at the minimum predicted operating temperature of 190 K, indium wire seals were used on the inner cell endplates, the gas-handling input bellows, and the inner cell vacuum port. Spring loaded PTFE seals were used for the CaF_2 windows, their housings and the shafts for the inner cell mirror adjustors. The housings for the mirror adjustors and the viewing windows were cemented in place with silicon rubber sealant. As the outer cell remained near room temperature, pernuban rubber O-rings and silicon rubber O-rings were adequate for the vacuum seals in this part of the LWC. The gas handling system for filling the cell with absorber gas mixtures utilised standard plumbing techniques for connecting cylinders of gas to the LWC. Because the LWC was intended for use with flammable gases, the gas handling and vacuum systems incorporated numerous safety features and interlocks which ensured that it was filled, monitored, and evacuated safely.

The windows are considered as part of the vacuum system, since their main function was to form gas-tight apertures through which radiation could pass. The LWC endplates were fitted with ports for mounting i.r. and viewing windows; i.r. windows were required only at the single-mirror end where they allowed radiation from the spectrometer to enter and leave the cell. Two i.r. windows were mounted in stainless steel housings that bolt to the inner cell endplate, and two were mounted in aluminium alloy housings attached to the endplate of the outer cell. A variety of windows could have been used depending on the application; for the work reported in Ref. 11, CaF_2 windows were used. Windows were typically wedged to prevent unwanted modulation of the beam by internal reflections.

The pressure rating of the windows was an important design parameter. For a crystalline material like CaF_2, the maximum stress, S_{max}, in a uniformly loaded circular plate of thickness t is given by (Marks[12]):

$$S_{max} = \frac{KD^2P}{4t^2} \tag{1}$$

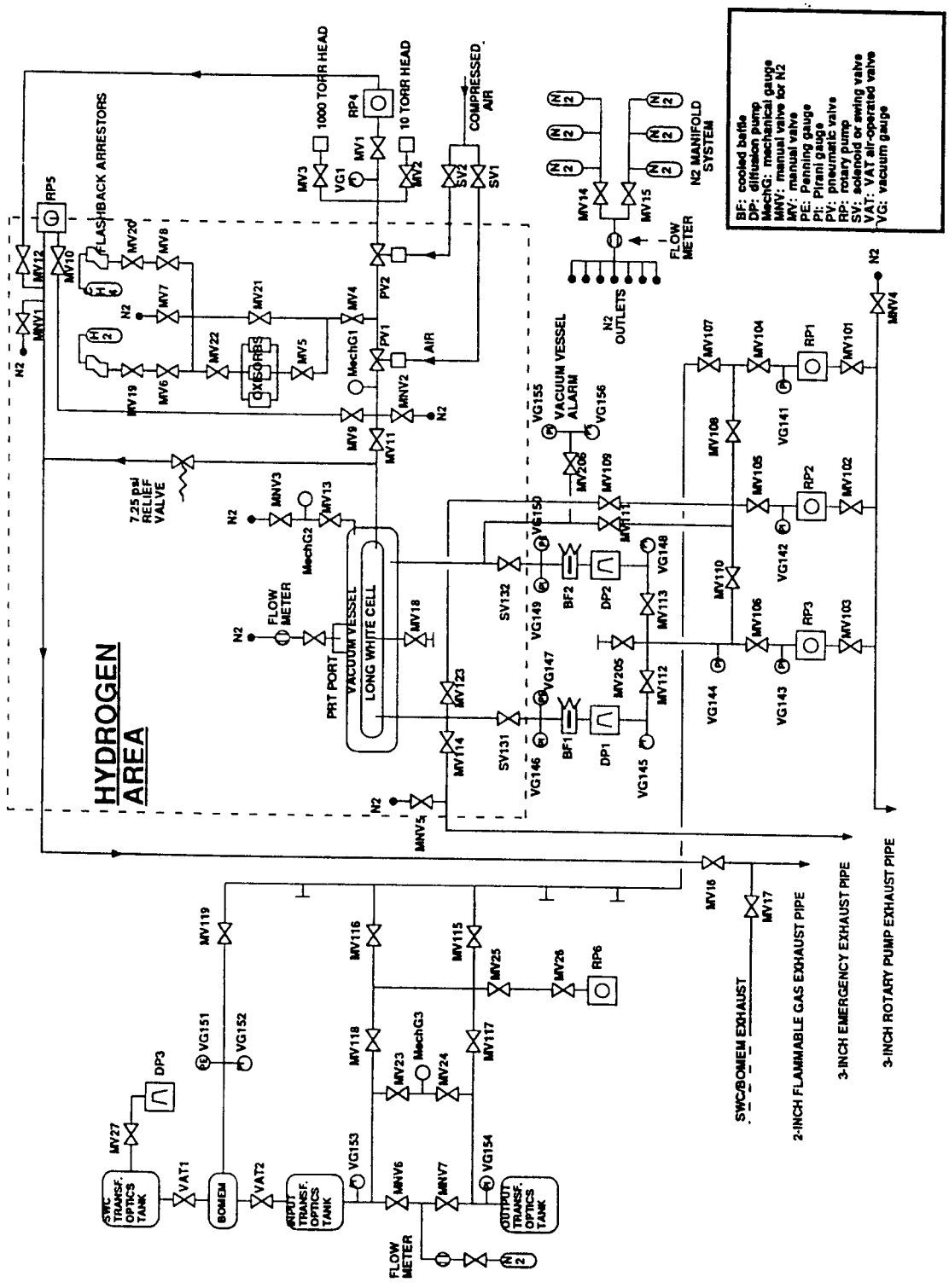

Fig. 2. Schematic diagram showing the layout of the LWC and the associated gas handling systems.

where K is a constant, dependent on the method of support, $=0.75$ for the clamped case and 1.125 for the unclamped case; D is the diameter of support; and P is the pressure differential across the window.

To avoid plastic deformation of crystal materials, S_{max} should be larger than the apparent elastic limit, F_a, by some safety factor, $SF > 1$. For the Ca_2F_2 windows, with $t = 5$ mm, $D = 60$ mm, $K = 1.125$ (worst case), $F_a = 3.654 \times 10^7$ N/m^2 (Ref. 13), a safety factor of 9 is obtained for a pressure differential of 1.0 bar.

Viewing windows were required through the inner and outer cell endplates at both ends of the LWC in order to allow the front surfaces of all three mirrors to be seen from outside the cell for optical adjustments. All eight windows were unwedged disks 12.7 mm thick and 125 mm in diameter, plate pyrex for the inner cell and plate glass for the outer cell. For these non-crystalline materials, F_a is the tensile strength, which is 6.3×10^7 N/m^2 for the pyrex and 16×10^7 N/m^2 for the glass. With $D = 115$ mm, these windows were rated to a pressure differential of 1.0 bar with a safety factor of 27 for the pyrex and 69 for the plate glass.

5. THE CRYOGENIC SYSTEM

The LWC cryogenic system, shown schematically in Fig. 3, was designed to allow the inner absorption cell temperature to be stepped between any two values in the range 190–300 K, and to be maintained at a given temperature for an extended period of time. The central feature of the system was the heat exchanger, which used LN_2 to cool a fluid circulated through a sealed circuit of cooling channels welded to the outer surface of the inner cell. The fluid used was Halon 2402, dibromotetrafluoroethane, which has a freezing point of 162.7 K. Although this is 86 K above the boiling point of LN_2, the speed with which the Halon 2402 was pumped through the heat exchanger prevented it freezing through the whole diameter of the pipe. The increasing viscosity of the Halon 2402 with decreasing temperature limited the lowest operating temperature of the LWC to 190 K. Replacing the Halon 2402 with a different heat exchange fluid, such as isopentane, will be necessary

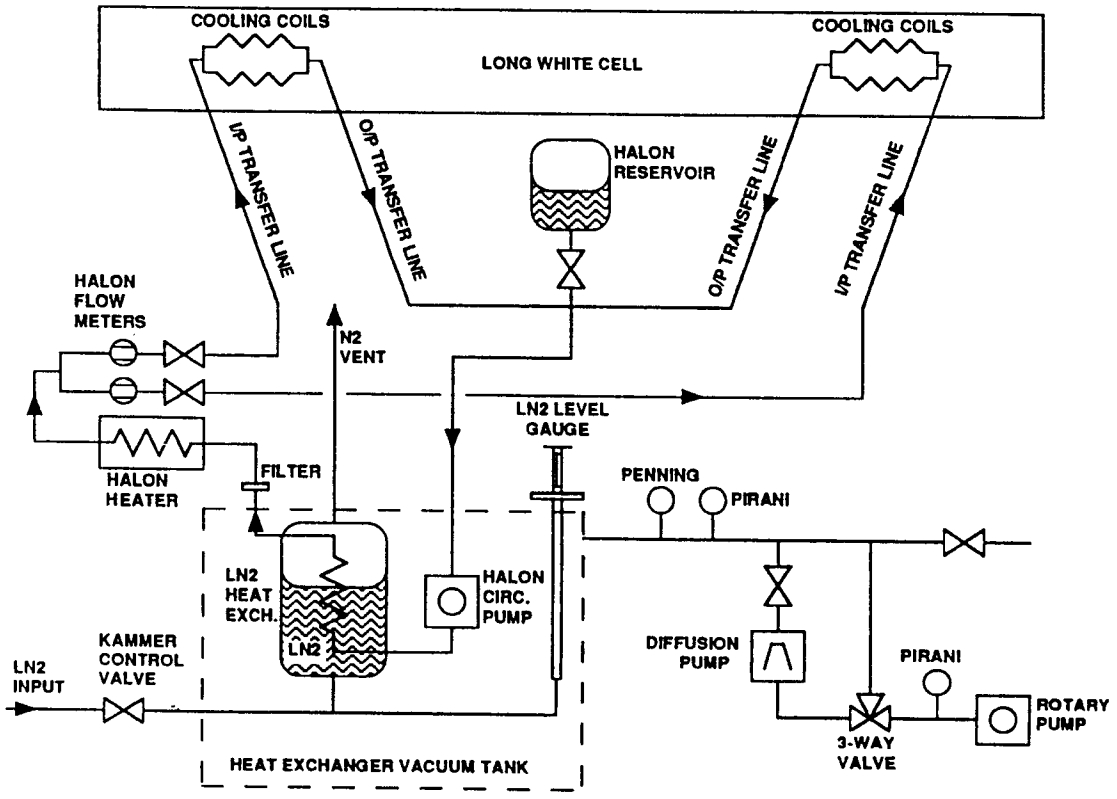

Fig. 3. Schematic diagram showing the arrangement for cooling the LWC.

for operation down to the lowest design temperature of 90 K, though this has not yet been implemented.

The heat exchange occurred in four double-walled vertical stainless steel pipes 400 mm in length, with outer diameters of 54.0 mm for the inner pipe and 66.7 mm for the outer pipe. LN_2 filled the central volume of the pipes and the Halon was contained in the surrounding annuli. The Halon was pumped through the system by a magnetic-drive centrifugal cryogenic pump which circulated the cooled fluid through the heat exchanger pipes, past two control valves into two vacuum-insulated transfer lines. Inserted in each transfer line was a flowmeter which provided digital readouts of the cooling-fluid flow rates. The lines led to two input ports on the top of the LWC, where the Halon passed through manifolds across the vacuum vessel into two independent cooling circuits. Each of these circuits consists of eight channels welded to the outer surface of the inner cell. The Halon returned to the heat exchanger through two output transfer lines. Also contained in the cooling-fluid circuit was a 3 kW heater which was used to speed up the rate of warming. Both the heat exchanger and the circulating pump were isolated within an insulating vacuum chamber which was maintained at a pressure $< 1 \times 10^{-6}$ mbar at room temperature. At 190 K, the pressure fell to $< 1 \times 10^{-7}$ mbar.

The LWC temperature control system comprised a LN_2 level sensor, a TCS 6382 microprocessor, and an air operated needle (Kammer) valve. The microprocessor, which received inputs from the LN_2 level gauge in the heat exchanger and from a platinum resistance thermometer located on the cooling-fluid circuit just beyond the output of the circulating pump, was programmed to maintain the LN_2 level in the heat exchanger or the cooling-fluid temperature at a specified setting. Conduction of heat between the inner and outer cells was reduced by the use of low-conductivity supports and connections, and conduction of heat by gas was minimised by operating with the outer cell evacuated. Heat input to the inner cell by radiation was reduced by multilayered interleaved aluminium foil and glass paper superinsulation wrapped around the outside of the inner cell and over its endplates, with appropriate holes cut for the windows and mirror adjustors.

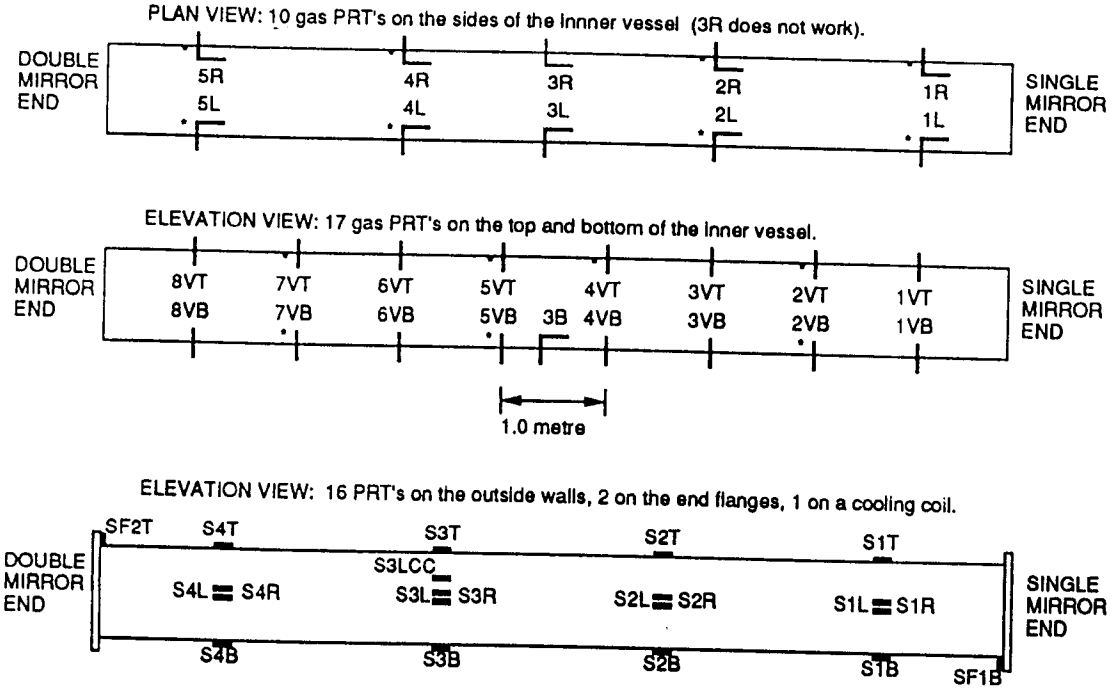

The "ed gas PRT's are those which were monitored with the data logger during the cold experiments.

Fig. 4. Schematic diagram showing the location of the PRTs in the LWC.

6. THERMODYNAMIC MONITORING OF THE GAS IN THE LWC

Temperatures in the LWC system were monitored at numerous points by 4-wire platinum resistance thermometers (PRT), supplied by Heraeus/Nulectrohms. Nineteen PRTs were clipped to the outer surface of the inner cell to monitor the temperature of the walls, and 27 PRTs were suspended inside the inner cell to monitor the temperature of the gas. The detailed construction of the PRT housing (length, diameter, wall thickness) was such that the gas PRTs measured the true temperature of the gas and were not influenced by the wall temperature. The location and orientation of the PRTs are shown in Fig. 4. The temperature of each PRT was determined using the fact that its electrical resistance is a known linear function of temperature, and is 100 Ω at 298 K. The resistance was determined by measuring the voltage across the PRT when a known d.c. current was passed through it, and applying Ohm's law.

The manufacturer's specified accuracy of the PRT temperature was ±0.1 K at 273 and 373 K, and ±0.3 K at 77 K. Heraeus/Nulectrohms performed a 3-point calibration on a sample of four of the gas sensors and two of the wall sensors, at these temperatures, and found that the specifications were satisfied. An additional 3-point calibration was performed at RAL, in November 1983, before the PRTs were installed in the LWC. This took the form of a check at room temperature and with the PRTs immersed in melting water ice, and LN_2. The pressure of gas in the LWC was measured with MKS Type 390 10 torr and 1000 torr Absolute Baratron Pressure Transducers. These sensors operate as capacitance manometers, having an internal circular inconel diaphragm whose deflection is a linear function of pressure, and which is mounted inside a thick-walled, temperature-controlled housing maintained at 318 K to reduce the influence of ambient temperature variations.

7. SAFETY CONSIDERATIONS

Numerous safety features have been incorporated into the LWC and ancillary equipment for the purposes of providing safe handling and containment of flammable gases and for recognising and dealing with escapes of these gases. Full details are given in Ref. 14, and here we give details of the main features only.

The LWC was located in an area specially designed for use with H_2 and other flammable gases (see Fig. 2), which is equipped with anti-static floor tiles, a frangible roof of polystyrene panels, sealed fluorescent lights, two extraction fans, and a flammable-gas detection system. The last consists of six detectors distributed around the area, which trigger both an audible alarm and an extraction fan when flammable gas is detected. The extraction fan outlet was fitted with a coronal shield to prevent the build-up of static charge. For the work described in Ref. 11, the detectors were set to detect 10% of the lower explosive limit of H_2 (4% H_2 in air). To eliminate the possibility of sparks all metal components were grounded and no electrical equipment was used in this area when flammable gas was present.

Evacuation of the cell was perceived as a particularly hazardous operation, so this was performed using a rotary pump (RP5 in Fig. 2) installed such that only the mechanical parts were located in the H_2 Area, with the electric motor outside. The exhaust line from this pump was simultaneously purged with N_2 gas. An Edwards E2M8 rotary pump was used for the room temperature experiments, and an E1M40 for the cold experiments, these taking 105 and 25 min respectively, to pump the inner vessel down from 760 to 20 torr. At 20 torr the flammable gas remaining in the cell was diluted with N_2 gas until the mixture was below the explosive limit (5% in air for CH_4 and 4% for H_2). This safe mixture was then removed with RP2 and DP1 (see Fig. 2).

All of the vacuum pump exhaust pipes were electrically grounded, and fitted with a non-return valve at the open end. For the CH_4 experiments, an alarm system was installed to alert the operators in the event of a fire in one of the vent pipes, or in the extraction fan pipe. This consisted of fusible links, mounted under tension at the outlet of each of these four pipes, wired to an electrical alarm.

The outer cell pumping system was not designed for use with flammable gas, and so was not used when flammable gas was contained in the inner cell in case a leak developed between the inner and outer cells. When the inner cell was cooled, the outer cell was evacuated and sealed prior to filling the inner cell with flammable gas. In addition, a pressure-rise alarm was installed on the outer

cell to warn of any such leaks. During the cold measurements, the pressure-rise rate was generally low enough to maintain cooling, but when a small leak developed between the inner and vacuum vessels, a noticeable increase in the LWC temperature-rise rate was observed, and it was sometimes necessary to rough out the outer cell on RP3 during the intervals between recording spectra. At room temperature the outer cell could alternatively be filled with 760 torr of O_2-free N_2.

8. ASSESSMENT OF PERFORMANCE OF THE LONG WHITE CELL

The LWC has been used at room temperature for several studies, including long-path spectroscopy of radicals (Ref. 15). It has also been used cooled during an extensive study of the spectroscopy of CH_4 and CH_4/H_2 mixtures (Ref. 11), and during the course of this work the operational performance of the LWC and the quality of the spectra recorded using it were examined critically. For these experiments, globar and quartz halogen sources and an InSb detector were used, and the iris aperture in the spectrometer was set to 1 mm diameter. Aspects of the performance assessment and spectral quality are discussed briefly below; a more extensive discussion can be found in Refs. 11 and 16.

8.1. Photometric performance

Before recording spectra, an assessment was made of the throughput of the cell at room temperature by recording the d.c. output from the InSb detector pre-amplifier as a function of pathlength. This output (after correction for the dark signal offset) was proportional to the intensity of radiation falling on the detector. This test was also used to ascertain the maximum useable pathlength (see Sec. 8.2). The results are shown in Fig. 5, in which the abscissa is the nominal pathlength (m), and the ordinate is the natural logarithm of the throughput, defined as the corrected pre-amplifier output at the set pathlength divided by the output at a pathlength of 64 m. If the only loss mechanism was reflection loss at the mirrors there would have been a linear relationship between log (throughput) and pathlength. Figure 5 demonstrates that this was the case for the LWC up to pathlengths around 320 m, and that for longer paths additional mechanisms, such as scattering and image distortion, became important. A straight line fitted to data points with pathlengths < 320 m gave an effective single-surface reflection coefficient of 0.977.

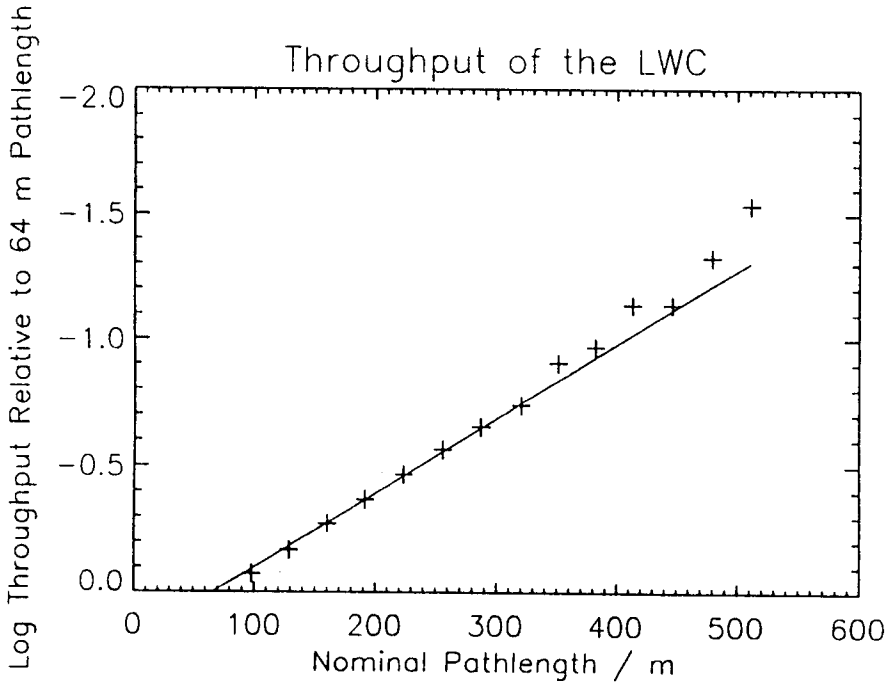

Fig. 5. Graph of $\log_e$ (throughput) against pathlength.

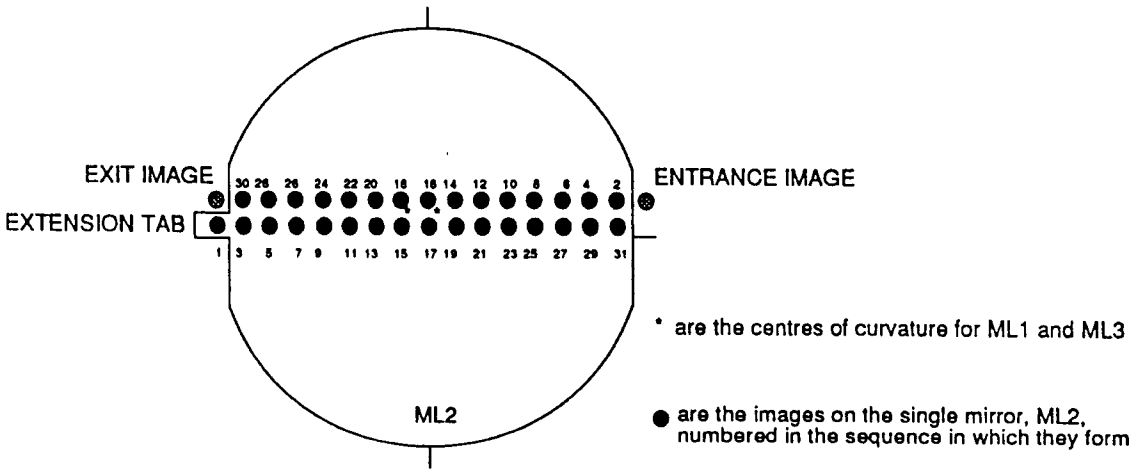

Fig. 6. Schematic diagram showing the ideal location of images on the LWC field mirror, and the order in which they are formed.

Spectra were obtained at 0.25 cm^{-1} resolution over the frequency range 2000–11,000 cm^{-1}. The noise in spectra recorded with the cryogenic circulating pump and the vacuum pumps turned off was similar to that in similar spectra recorded through the spectrometer sample compartment. The noise increased to an unacceptable degree with the circulating pump and certain vacuum pumps operating, due to mechanically-induced vibration of the LWC mirrors, and for this reason these pumps were always switched off during data collection. Spectral transmittances were derived by dividing spectra recorded with gas in the cell by spectra recorded with the cell evacuated. In these spectra, regions of zero absorption should ideally have unity transmission, but in many cases this was not so. This discrepancy was due to several factors which could be attributable to the LWC. The signal level was observed to be particularly sensitive to the alignment of the LWC mirrors, and particularly to the position of the first image on the tab, so that small changes in alignment due to the presence of gas in the LWC, mirror movement, or temperature drift, could cause systematic changes in the signal. The signal level also fluctuated when gas was introduced into the LWC, the turbulence and change in pressure apparently causing slight changes in the index of refraction of the gas. When using the cell at 240 and 190 K, the mirrors were adjusted after each gas fill in order to maximise the signal, but it was not always possible to regain the previous signal level (discounting the expected decrease due to gas absorption). Systematic drifts in the background spectra were also observed. One apparent cause was a relaxation of the LWC mirror adjustors and this could sometimes be reduced by disengaging the outer handles. The procedures adopted for dealing with these deviations are discussed in Ref. 11.

8.2. Pathlength adjustments

Pathlengths in metres were given by the expression $L = 0.75 + 16 \times (n + 1)$, with a cumulative uncertainty of $0.02 \times (n + 2)$ m, where n is the number of images on the field mirror. The 0.75 m represents twice the distance from the inner surface of the i.r. windows to the front surface of the field mirror at its edge. Pathlengths in excess of 32.75 m were achieved by positioning the first image on the field mirror tab and subsequent images on the main portion of the field mirror. The longest path used had 30 images on the field mirror, in addition to the image on the tab. The ideal positioning of the images and the order in which they are formed is shown in Fig. 6. The longest useable pathlength was determined by observing the output from the detector as the pathlength was increased. Initially this was seen to fall to zero between successive maxima which indicated that the LWC output image was well focussed on the detector. However for pathlengths greater than 512 m the signal did not fall completely to zero indicating that the images on the field mirror were beginning to overlap. This is a consequence of image spread due to abberations, diffraction, and scattering. Aberrations fundamental to the White optical design and its variants have been discussed by several authors (e.g., Kohn,[17] Hannan,[18] Reesor[19]), and are principally spherical

aberration and/or astigmatism. For our experiments the cell optics were adjusted to give maximum detector output, so it is likely that both spherical abberation and astigmatism were present.

During the course of the experiments, difficulties were encountered with several aspects of the pathlength adjustment and determination. The pathlength was determined by counting the number of images on the field mirror with the aid of a telescope arranged to view the field mirror through a viewing window at the opposite end of the cell. With this arrangement the images were relatively easy to count initially, though after some time operating the cell cold a misty film of oil condensed on the viewing windows which made it impossible to see the faintest images. This problem was solved to a large extent by replacing the oil diffusion pump on the outer cell with a turbomolecular pump, and by re-siting a cryogenic baffle.

The mirror adjuster rods, which initially became scratched during rotation and disengagement, caused difficulties in pathlength adjustments. These problems were overcome by making the rods from phosphor bronze rather than stainless steel and by increasing the diameter of the holes through which the rods passed. Lubrication of the adjustors and moving mechanisms in the mirror mounts also proved to be necessary for trouble free pathlength adjustments, as all of the mirror adjustors seized up during one of the LWC cooling tests. Thereafter a molybdenum disulphide lubricant was applied to all moving parts in the mirror adjustors, and no further problems from this source were encountered.

8.3. Cryogenic performance and temperature measurements

The LWC was cooled by operating the microprocessor controller in a mode whereby it initially applied full cooling power until the controlling PRT indicated a pre-set temperature, at which point it applied a variable cooling power to maintain the set temperature. This was done by varying the level of LN_2 in the heat exchanger. The temperature of the cell during cooling to ~ 190 K is shown in Fig. 7. The LN_2 consumption was ~ 100 l/h during cooling, and ~ 20 l/h during operation at 190 K. The temperature rise rate of the LWC with the circulating pump turned off was ~ 1 K/h. This was an important parameter since it was found that the pump caused unacceptable vibration

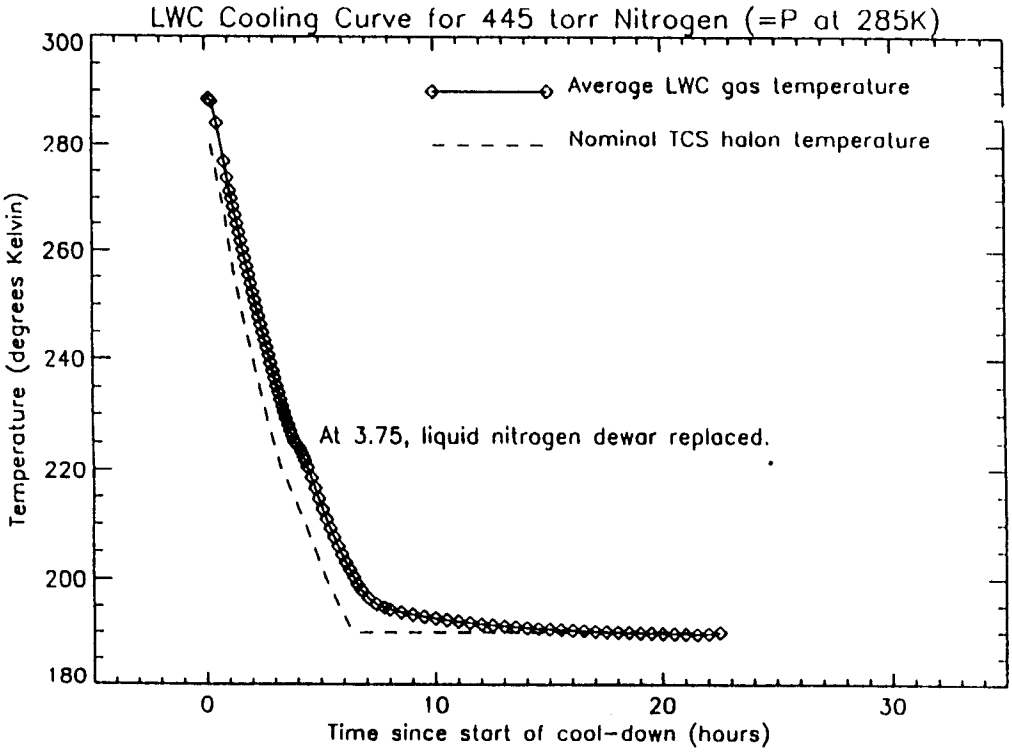

Fig. 7. A cooling curve for the LWC which contains N_2 gas initially at 593 mbar and 285 K.

Table 2. Table comparing measured gas temperatures with gas temperatures derived assuming ideal gas behaviour on cooling the LWC from near 296 K to near 240 K.

	MEASURED $T_o \pm 1\sigma$ (K)	MEASURED $T_f \pm 1\sigma$ (K)	CALCULATED T_f (K)	ΔT_f (K) (CALC - MEAS)
Current source (26 gas PRTs)	294.5 ± 0.2	241.5 ± 2.2	243.2	+ 1.7
Data recorder (15 gas PRTs)	294.1 ± 0.2	241.1 ± 1.7	242.9	+ 1.8
Average ΔT (current source – data recorder)	+ 0.4	+ 0.4		

of the LWC during spectral measurements (Sec. 8.1), and so spectra were recorded with it turned off.

The LWC temperatures were monitored using PRTs, as described in Sec. 6. A 15 channel Phillips PM8237A/02 Multipoint Data Recorder was used to measure the PRT resistances using an internal 0.7685 mA current source, and conversion to temperature was done internally with the DIN 43760 linearisation scale. Tests of all 15 of the data recorder channels, using a precision variable resistor, showed that the difference between temperatures from the data recorder and those calculated directly from the resistances using the DIN 43760 scale were always less than ±0.2 K and therefore within the specified accuracy of the recorder. The overall uncertainty of the temperature measurements when the LWC was cooled (ΔT), aside from the variation due to temperature gradients in the LWC, was the sum of the quoted accuracy of the PRTs (±0.3 K) and the accuracy of the data recorder. Thus $\Delta T = \pm(0.7 + 0.001 \times T_{IN})$, where T_{IN} is in degrees Celcius, and a room temperature of 20°C is assumed.

Because the data recorder had only 15 channels, it was necessary to choose a representative set of PRTs for routine monitoring. This included all those along the left and right sides of the LWC (1R, 2R, 4R, 5R, 1L, 2L, 4L, and 5L, excluding 3R because it was broken and 3L because it gave consistently high readings—see Fig. 4) as these were at approximately the same height as the optical path. Of the vertical sensors, a 2VT, 2VB, 4VT, 5VT, 5VB, 7VT, and 7VB were chosen, these being fairly evenly distributed along the length of the LWC. The data recorder was programmed to record the temperatures every 10 min. In addition, PRT 6VT was connected to an independent constant current (~1 mA) source, and the voltage across the PRT was recorded on a chart recorder.

The accuracy of the PRT readings at low temperature was further evaluated by measuring the temperature and pressure of the gas in the LWC during cooling and comparing it with ideal gas behaviour. The LWC was filled with 801 mbar of N_2 gas at room temperature, and PRT readings were recorded using both a separate 1 mA constant current source for all 26 gas PRTs, and using the data recorder for the 15 selected gas PRTs. As a check on the reliability of the measurement of the initial temperature, T_0, the current source was also used to measure the average room temperature of the 17 wall PRTs, which was found to be 294.4 ± 0.2, in good agreement with the values for the gas PRTs. The LWC was then cooled and 6 h later, when the pressure had dropped to 662 mbar, the temperatures were recorded again. The average measured temperatures and their standard deviations are displayed in Table 2, along with the calculated final temperatures, T_f.

This test showed that the measured PRT cold temperatures were colder than the theoretical values, by 1.7 K for the current source, and by 1.8 K for the data recorder. These differences are comparable to the standard deviations in the measured cold temperatures, these being 2.2 and 1.7 K, respectively. The accuracy of the low-temperature PRT readings was therefore considered acceptable. The slight cold bias of the measured T_f relative to the calculated value suggests that there may be warm pockets in the LWC which contribute to the overall temperature but are not registered by any PRTs. This is supported by the fact that PRTs 3L, 3B, and 4VB, near ports midway along the inner vessel, gave consistently higher temperatures, apparently due to heat leaks through the ports. The results in Table 2 also show that both the room and cold temperatures measured with the data recorder were 0.4 K lower than those measured with the current source. This small cold bias of the average temperature measured by the data recorder relative to the average temperature measured using the independent current source suggests that the 15 PRTs

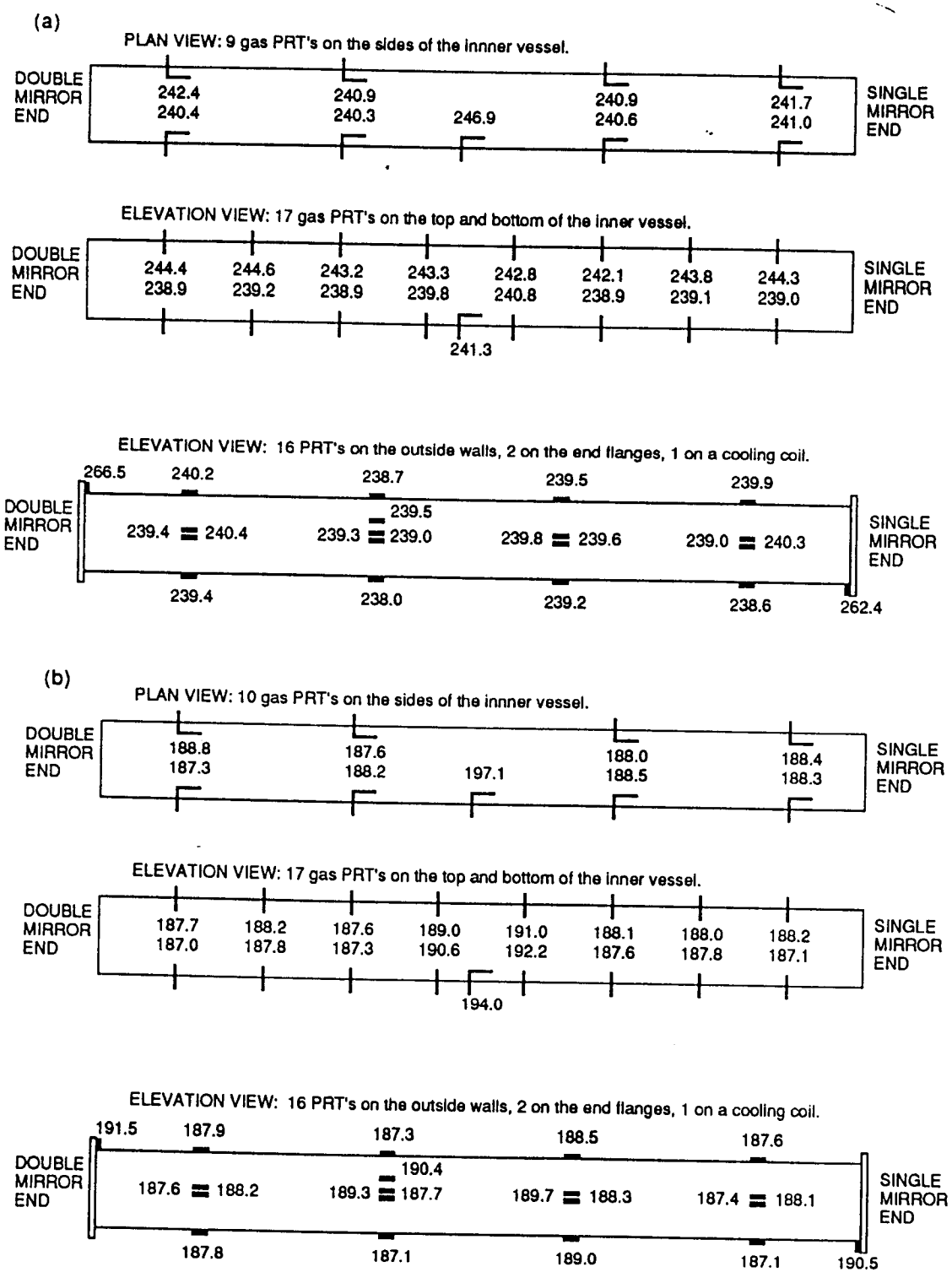

Note: this PRT map was recorded 6 hours after the start of cooling from an initial LWC temperature of 294 K. The pressure of nitrogen in the LWC was 496.4 torr when these temperatures were recorded.

Fig. 8. Temperature maps for the LWC at nominal temperatures. (a) 240 K and (b) 190 K.

chosen for the data recorder were not fully representative of the 26 gas PRTs. A similar small bias was also seen in several other tests, but the discrepancies were always within the instrumental uncertainty of the data recorder and were therefore considered acceptable.

An indication of the temperature distribution through the LWC when filled with gas at nominal temperatures of 240 and 190 K can be obtained from Fig. 8, which shows the temperatures indicated by various PRT sensors once the LWC temperature had stabilised.

8.4. Vacuum and gas handling systems, and pressure measurements

Referring to Fig. 2, rotary pump RP2 was used to rough out the inner and outer cells, taking ~25 min for the former and up to 24 h for the latter (due to outgassing from the superinsulation), assuming that the system had been purged with dry nitrogen. The diffusion and turbo-molecular pumps could easily maintain pressures $< 10^{-5}$ mbar in these cells. When the inner and outer cells were evacuated and isolated the maximum room temperature pressure-rise rates were measured to be $\sim 9 \times 10^{-4}$ mbar/h for the inner cell (with 950 mbar of N_2 in the outer cell), and $\sim 7 \times 10^{-5}$ mbar/h for the outer cell (with 950 mbar of N_2 in the inner cell). RP5, an Edwards model E1M40, was used to rough out the inner cell to a pressure of 27 mbar when it contained flammable gas. This operation took 25 min from an initial pressure around 1000 mbar. The gas handling systems performed to their design requirements.

Gas sample pressures were measured using Baratron capacitance manometers. The 10 torr and 1000 torr heads were calibrated by MKS Instruments before being installed in the gas-handling system, and both were found to be accurate to within 0.04%. Periodic checks of the 1000 torr head were also made comparing measurements of atmospheric pressure with that measured using a precision aneroid barometer. The baratron was found to read as much as 0.09% higher than the aneroid barometer, which was slightly worse than the specified calibration error for the baratron. The consistency of readings from the two baratron heads at five pressures over the range from 0 to 10 torr was also checked periodically, and a maximum difference of 1.1% was observed. The individual pressure measurements were therefore considered to be accurate to at least 1.1%.

During the experiments described in Ref. 9, the LWC was kept isolated as much as possible when full of flammable gas. The method of operation was to record the LWC pressure immediately after filling, then to isolate the LWC at PV1 and remove gas from the gas handling system while spectra were being recorded, and finally to record the LWC pressure again once collecting spectra was finished. The intermediate pressures were then linearly interpolated from the initial and final pressures.

9. CONCLUSIONS

A gas cell with which absorption spectra can be recorded over a wide range of temperatures, pressures, and pathlengths has been installed at the Rutherford Appleton Laboratory and interfaced to a Bomem DA3.002 spectrophotometer. Practical features of the cell include pathlengths up to 512 m, temperatures down to 190 K, pressures up to 5 bar and the capability to work with corrosive and flammable gases. The cell has recently been used to record an extensive set of spectra of CH_4 and H_2, both separately and mixed. The practical performance of the cell/spectrometer system has been assessed during the course of this work and the main aspects have been reported here.

Acknowledgements—The authors wish to thank all the technical staff at the Rutherford Appleton Laboratory who have contributed to the designing, building, and commissioning of the Long White Cell, in particular P. Pennington and G. Pullinger. This work was funded by the U.K. Science and Engineering Research Council.

REFERENCES

1. H. J. Bernstein and G. Herzberg. *J. chem. Phys.* **16**, 30 (1948).
2. E. E. Stephens, *Infrared Phys.* **1**, 187 (1961).
3. R. P. Blickensderfer, G. E. Ewing, and R. Leonard, *Appl. Opt.* **7**, 2214 (1968).
4. A. R. W. McKeller, N. Rich, and V. Soots, *Appl. Opt.* **9**, 222 (1970).

5. D. Horn and G. C. Pimentel, *Appl. Opt.* **10,** 1892 (1971).
6. R. Le Doucen, J. P. Houdeau, C. Cousin, and V. Menoux, *J. Phys. E* **18,** 199 (1985).
7. R. E. Shetter, J. A. Davidson, C. A. Cantrell, and J. G. Calvert, *Rev. Scient. Instrum.* **58,** 1427 (1987).
8. K. C. Kim, E. Griggs, and W. B. Person, *Appl. Opt.* **17,** 2511 (1978).
9. R. A. Breismeister, G. W. Read, K. C. Kim, and J. R. Fitzpatrick, *Appl. Spectrosc.* **38,** 35 (1984).
10. J. U. White, *J. opt. Soc. Am.* **32,** 285 (1942).
11. K. Strong, F. W. Taylor, S. B. Calcutt, J. J. Remedios, and J. Ballard, *JQSRT* **50,** 363 (1993).
12. L. S. Marks, ed., *Mechanical Engineer's Handbook*, 4th edn, McGraw-Hill, New York (1941).
13. *B. D. H. Crystran Crystals Handbook*, B. D. H. Ltd (1988).
14. K. Strong, Rutherford Appleton Laboratory Report RAL-91-015 (1991).
15. P. T. Wassell, R. P. Wayne, J. Ballard, and W. B. Johnston, *J. atmos. Chem.* **8,** 63 (1989).
16. K. Strong, D. Phil. thesis, Oxford University (1992).
17. W. H. Kohn, *Appl. Opt.* **31,** 6757 (1992).
18. P. Hannan, *Opt. Engng* **28,** 1180 (1989).
19. T. R. Reesor, *J. Opt. Soc. Am.* **41,** 1059 (1951).